Signature of on-off intermittency in measured signals

Chiara Toniolo*
Doctorate Program in Environmental Engineering Fluid Dynamics, University of Genova, Genova, Italy

Antonello Provenzale*
Institute of Atmospheric Sciences and Climate, Corso Fiume 4, I-10133 Torino, Italy

Edward A. Spiegel
Department of Astronomy, Columbia University, New York, New York 10027

(Received 5 September 2001; revised manuscript received 3 September 2002; published 18 December 2002)

On-off intermittency is a phase-space mechanism that allows dynamical systems to undergo bursting. As its name suggests, bursting is a phenomenon in which episodes of high activity are alternated with periods of inactivity. Here we attempt to see whether we can tell from the output of a signal when an observed bursting behavior is caused by the presence of on-off intermittency, using the example of a forced logistic map. The results of our study indicate that on-off intermittency can be readily distinguished from other mechanisms for bursting we know of, except for one. Many statistical properties of finite-length signals generated by on-off intermittency can in fact be mimicked by the output of a nonlinearly filtered, linear autoregressive random process.

DOI: 10.1103/PhysRevE.66.066209 PACS number(s): 05.45.−a, 07.05.Kf

I. INTRODUCTION

In 1949, Batchelor and Townsend used the word *intermittency* to describe their observations of the patchiness of the fluctuating velocity field in a fully turbulent fluid [1]. The kind of intermittent behavior isolated in their observations occurs whenever systems alternate continually between bursts of activity and quiescent states. Many natural systems display such behavior. Solar activity is an example of current interest [2,3] because its cyclic production of sunspots suffers sporadic interruptions that may be associated with cold weather on earth. In the laboratory, Maurer and Libchaber [4] have produced records of temperature variation at a point in a thermally convecting fluid that clearly exhibits the phenomenon. These two examples must serve to represent the many known occurrences of vacillation between high excitation and dormancy that are too numerous to list here.

In the past twenty years, the term intermittency has come to be used to refer to a wider class of alternations in behavior, as between temporal almost periodicity to continuous chaos. With the proliferation of models to explain such variations, workers in dynamical systems theory have realized that there are many different kinds of phase-space mechanisms that produce intermittency, especially of purely temporal behavior. For example, an early and readily visualized mechanism of such alternation is the Pomeau-Manneville scenario for the behavior of a system in the proximity of a saddle-node bifurcation [5]. A different mechanism, which is the subject of the present paper, is the one called *on-off intermittency*, see Ref. [6] for an introduction to this type of dynamics and Ref. [7] for an early discussion of bursting dynamical systems. More recently, several discussions of bursting mechanisms have been published [8–14]; some of these are variants of the on-off mechanism and some appear to be distinct. To avoid confusion, we shall adopt here the somewhat imprecise term *bursting* to describe the observed behavior that the various models are trying to capture, and retain the term on-off intermittency for the particular mechanism that we study here.

A first question that we consider in this paper is how to determine in which regions of parameter space on-off intermittency may occur. As we see below for the model studied here, on-off dynamics is confined to a narrow region in parameter space, at the border between ordered behavior and full-blown noise-driven chaos so that passage through on-off intermittency is one route to chaos.

A further question that we address is how to tell whether a given bursting behavior is well modeled by the specific process of on-off intermittency, as opposed to other possible mechanisms (such as the Pomeau-Manneville mechanism). In this work we thus analyze some of the observable statistical properties of the on-off intermittency mechanism, continuing along the lines of Heagy *et al.* [15]. The goal of this effort is to obtain a sufficiently refined characterization of on-off intermittency that will permit us to detect it (or rule it out) in time-series data. As we have shown elsewhere [16], and we discuss further here, this is often a difficult task in time-series analysis. We shall illustrate the procedure with a simple model whose output is easily calculated.

II. THE DRIVEN LOGISTIC MAP

In the interests of ease of computation and clarity of exposition we concentrate here on the simple example of the driven logistic map,

$$X_{t+1}=A(Y_t)X_t[1-X_t]. \tag{1}$$

The quantity $A(Y_t)$ is to be specified but we assume that $0 \leqslant A \leqslant 4$ and that it is a *monotonic* function of Y_t. This sys-

*Also at ISI Foundation, Viale S. Severo 65, I-10133 Torino, Italy.

tem has the invariant manifold $X=0$ and we shall measure the level of activity of the system by $|X_t|$.

In the simple case where the dynamics of Y_t does not depend on X_t, we have a skew-product structure and it is then relatively easy to anticipate what kind of qualitative behavior the model will produce. If we freeze Y_t the stability of $X=0$ is decided by the instantaneous value of A. In the state of frozen Y_t, the map may have a second fixed point away from $X=0$. When A drops below unity, this point ceases to exist and the system heads back toward $X=0$, there to hover quiescently with $|X_t|$ close to 0 until A rises above unity once again. Though the detailed behavior to be expected when there is no skew-product structure is harder to anticipate, numerical studies show that on-off intermittency occurs robustly. In either case, to produce marked bursting, we need the invariant manifold to be sufficiently attracting during sufficiently long stable phases. As we see below, this happens in only a small portion of the available parameter space that represents a transition from order to chaos.

To see the on-off mechanism in action, we specialize to the explicit case of a noise-driven logistic map, with

$$A(Y_t)=A_0+\alpha Y_t, \tag{2}$$

where Y_t is δ-correlated noise that is uniformly-distributed in the interval $[0,1]$ and A_0 and α are parameters. To ensure that $0\leqslant A(Y_t)\leqslant 4$, we restrict ourselves to the case $A_0\geqslant 0$, $\alpha\geqslant 0$, and $A_0+\alpha\leqslant 4$. Figure 1 shows the parameter plane for the noise-driven systems (1) and (2). The dark gray area indicates the parameter range for which the fixed point $X=0$ is stable. The pale gray area indicates the parameter range for which the point $X=1-1/A$ would be attracting if A were constant. Outside the two gray regions in parameter space, the system undergoes different types of noisy chaotic dynamics.

The intermittent dynamics of systems (1) and (2) has been described in Refs. [6,15,17]. Bursting is observed in the temporal evolution of X_t as the stability of the fixed point $X=0$ varies. Figure 2(a) shows a time series of X_t for the parameter values $A_0=0$ and $\alpha=2.75$. Heagy *et al.* [15] have shown that for $A_0=0$ there is a critical value $\alpha_c>1$, below which the system asymptotically tends to the fixed point $X=0$, without any sustained intermittent bursting. Such a critical value exists also for $0<A_0<1$, leading to a critical line $\alpha_c(A_0)>1-A_0$ that separates a region with no intermittency for $\alpha<\alpha_c$ from a region where on-off intermittency is possible, for $\alpha>\alpha_c$.

To derive the critical line (following Heagy *et al.*), we recall that the bursting behavior is determined by the linear instability of the systems (1) and (2). For prescribed $A(Y_t)$, the linear equation in proximity of the fixed point $X=0$ can be written as

$$X_{t+1}=A(Y_t)X_t+O(X_t^2), \tag{3}$$

and thus we can write

$$\ln\frac{X_{t+1}}{X_0}\approx\sum_{r=0}^{t}\ln A(Y_r)=(t+1)\langle\ln A\rangle, \tag{4}$$

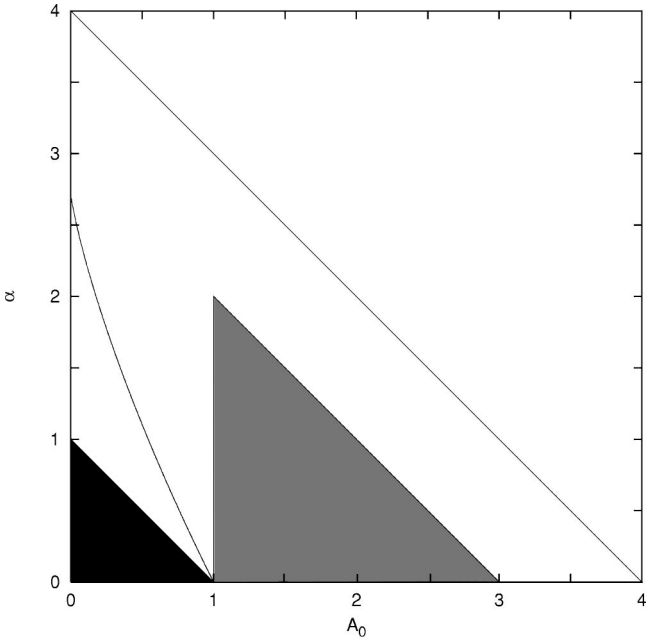

FIG. 1. Parameter plane for the stochastically forced systems (1) and (2) discussed in the text. Allowed values of the parameters A_0 and α must satisfy $A_0+\alpha\leqslant 4$ (this limit is indicated by the solid curve at $-45°$). The dark gray area indicates the parameter range for which the fixed point $X=0$ is stable. The pale gray area indicates the parameter range for which the point $X=1-1/A$ would be attracting if A were constant. The curve on the lower left indicates the minimum parameter values, Eq. (9), for which on-off intermittency is present; below this curve the system tends to the fixed point $X=0$.

where the angular brackets indicate time average over the interval $[0,t]$. Then

$$X_{t+1}=X_0\exp[(t+1)\langle\ln A\rangle]. \tag{5}$$

In the case $\langle\ln A\rangle>0$, the fixed point $X=0$ becomes unstable. For $\langle\ln A\rangle<0$, the fixed point is stable and the bursting behavior, even if present, is just a transient. With Eq. (2), we then find that the value of α_c for which

$$\langle\ln(A_0+\alpha_c Y_t)\rangle=0 \tag{6}$$

is the approximate marginal stability curve for the onset of on-off intermittency.

The value of $\langle\ln A\rangle=\langle\ln(A_0+\alpha Y_t)\rangle$ depends on the probability distribution of Y_t, which we denote as $\rho(Y)$. For the uniformly distributed random noise considered above, $0\leqslant Y<1$, $\rho(Y)=1$, whence

$$\langle\ln(A_0+\alpha Y_t)\rangle=\int_0^1 dY\rho(Y)\ln(A_0+\alpha Y) \tag{7}$$

and so

$$\langle\ln A\rangle=\frac{1}{\alpha}[(A_0+\alpha)\ln(A_0+\alpha)-A_0\ln A_0-\alpha)]. \tag{8}$$

Thus, the critical condition, $\langle\ln A\rangle=0$, is given by

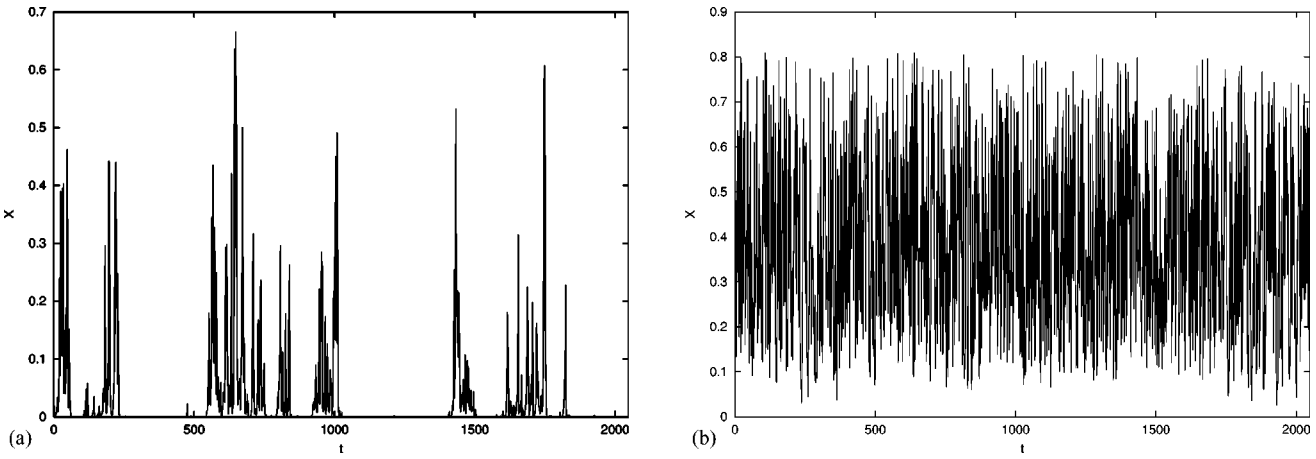

FIG. 2. Sample time series of the driven variable X_t in the stochastically forced systems (1) and (2) for the parameter values (a) $A_0=0$, $\alpha=2.75$; (b) $A_0=0.5$, $\alpha=2.75$.

$$(A_0+\alpha_c)\ln(A_0+\alpha_c)-A_0\ln A_0-\alpha_c=0. \tag{9}$$

This implicitly defines $\alpha=\alpha_c(A_0)$, shown as a curve in Fig. 1. However, $\alpha>\alpha_c$ is only a necessary condition for on-off intermittency. As we show below, on-off intermittency exists only in a limited region of parameter space just above this curve. For example, Fig. 2(b) shows a time series of X_t for the parameter values $A_0=0.5$ and $\alpha=2.75$, above the critical line. This time series does not display on-off intermittency, as we shall see, and the system undergoes noisy chaotic dynamics. In the following, we use the two signals shown in Fig. 2 to contrast intermittent dynamics with noisy chaotic, nonintermittent behavior. This will allow for better characterizing the properties of this mechanism for bursting and for determining the region of parameter space where on-off intermittency can be found.

III. A POWER-LAW TALE

In this section we consider the two examples of the systems (1) and (2) corresponding, respectively, to behaviors that are intermittent, as shown in Fig. 2(a), or noisy chaotic, as in Fig. 2(b). Our goal is to isolate the properties of on-off intermittency and to learn to detect on-off intermittency in measured time series by using the simple example of the noise-driven logistic map. As we show in the following, on-off intermittency is closely associated with power-law statistics.

A. Signal amplitudes

Figure 3(a) shows the amplitude probability density function, $\varpi(X)$, for the intermittent and nonintermittent cases discussed above, corresponding, respectively, to the parameter values $(A_0=0,\alpha=2.75)$ and $(A_0=0.5,\alpha=2.75)$. The distributions have each been computed from an ensemble of 100 realizations of the process. For every realization we used a different seed for the random number generator (to obtain a different sequence of random numbers in the stochastic driver), and we produced a time series of $2^{17}=131\,072$ points. The intermittent system always resulted in a power-law distribution of the signal amplitude.

Close to the critical curve above which on-off intermittency appears, the signal amplitude has a distribution $\varpi(X)\propto X^{-1}$ for X less than about 0.1. For larger values of X, the distribution deviates from a power law. The behavior of the amplitude distribution at small X can be understood by considering the linearized dynamics of systems (1) and (2), already discussed for the derivation of the critical curve for on-off intermittency. For small values of X_t and $A_0=0$, we can write

$$X_{t+1}\approx\alpha Y_t X_t=\alpha X_0\prod_s Y_s. \tag{10}$$

Thus, from the relationship

$$\varpi(X)dX\propto P\left(\prod_s Y_s\right)d\prod_s Y_s \tag{11}$$

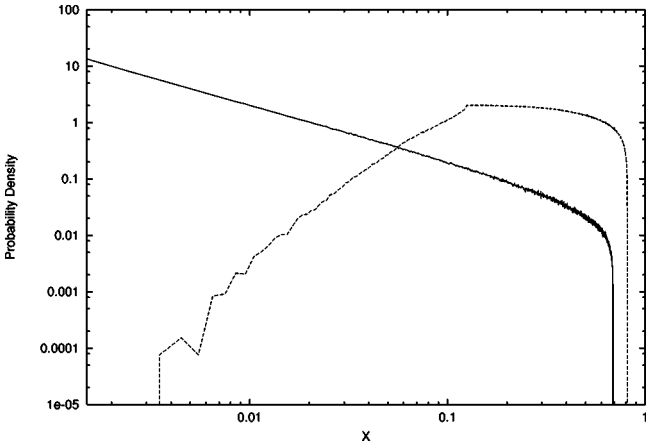

FIG. 3. Amplitude distribution for the on-off intermittent dynamics corresponding to $A_0=0$, $\alpha=2.75$ (solid line) and for the nonintermittent dynamics corresponding to $A_0=0.5$, $\alpha=2.75$ (dashed line). The distributions have been obtained by an average over 100 realizations of the process. Each realization has a length of 2^{17} points.

and Eq. (10) we obtain that $\varpi(X) \propto P(\Pi_s Y_s)$, where $P(\Pi_s Y_s)$ is the distribution of $\Pi_s Y_s$. Then we may introduce a new probability density $\tilde{P}$ and write

$$P\left(\prod_s Y_s\right) d\prod_s Y_s \propto \tilde{P}\left(\sum_s \ln Y_s\right) d\sum_s \ln Y_s . \quad (12)$$

Hence

$$\varpi(X) \propto \tilde{P}\left(\sum_s \ln Y_s\right) \frac{d \ln \prod_s Y_s}{d\prod_s Y_s} \propto \tilde{P}\left(\sum_s \ln Y_s\right) X^{-1}, \quad (13)$$

where the factor $\tilde{P}(\Sigma_s \ln Y_s)$ introduces only lognormal corrections. This simple, but general, argument rationalizes our numerical findings.

Owing to the power-law distribution, for on-off intermittent signals the kurtosis

$$k_X = \frac{\langle (X_t - \langle X \rangle)^4 \rangle}{\langle (X_t - \langle X \rangle)^2 \rangle^2} \quad (14)$$

of the amplitude distribution is significantly larger than the Gaussian value $k_g = 3$. For nonintermittent, randomly driven chaotic states, on the other hand, we find values of the kurtosis that are close to 3.

B. On and off phases

A measure of intermittency that is used in the study of turbulence is the fraction of time the system is in the active state, or intermittency factor. The term duty cycle also appears in such contexts. However, in their study of on-off intermittency in the systems (1) and (2), Heagy *et al.* preferred to measure the time spent in the quiescent, or off, state. They found that the probability of having an off, or laminar, phase lasting a time T_ϕ is proportional to $T_\phi^{-3/2}$. In measuring the durations of on and off phases, we need to specify an amplitude of activity, X_C, above which the system is considered to be on. For the choice $X_C = 0.001$, Fig. 4 shows the distribution of off, or laminar, phases for the intermittent case, as obtained from a time series with length $T = 2 \times 10^7$. Bursting behavior is associated with a power-law distribution of durations of the off phases, for a large range of thresholds. By contrast, the stochastically driven, nonintermittent chaotic dynamics produces completely different signals. Clearly, there are no discernible off phases for the nonintermittent chaotic state, as the system never remains long in or near to the invariant manifold in which it is considered to be in the off state. One could, however, define the state of being off as characterized by $|X_t - \langle X \rangle| < C$, where C is a suitably defined constant and $\langle X \rangle$ is the time average of X_t, or similarly by $|X_t - (1 - A^{-1})| < C$ for $A > 1$. In both cases, no scaling emerges and the durations of the off phases defined in this way have a distribution that falls off rapidly. An example is provided in Fig. 4, where we show the distribution of the duration T_ϕ of the phases for which $|X_t - \langle X \rangle| < 0.001$, for the nonintermittent case corresponding to $A_0 = 0.5$ and $\alpha = 2.75$. This distribution drops off much more rapidly than $T_\phi^{-3/2}$.

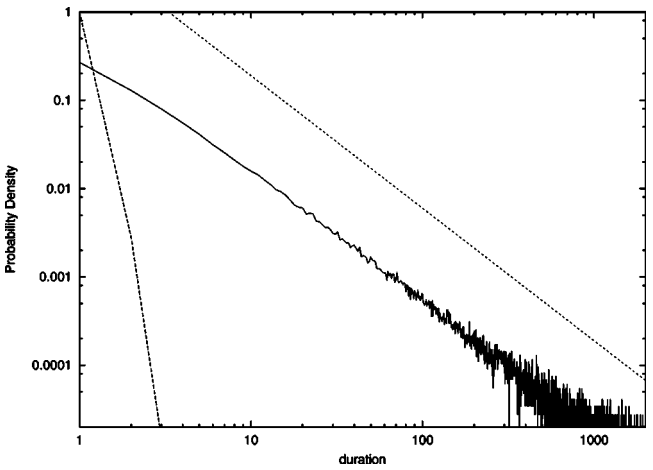

FIG. 4. Distribution of the duration T_ϕ of the *off* phases for the intermittent case, corresponding to $(A_0 = 0, \alpha = 2.75)$ (solid line), and for the nonintermittent case, corresponding to $A_0 = 0.5$, $\alpha = 2.75$ (dashed line on the left). The upper dot-dashed line indicates a power-law behavior $T_\phi^{-3/2}$. The distributions have been obtained from realizations of length 2×10^7 points.

The properties of the distribution of the off phases do not depend on the global properties of the specific system considered, but are generated by the dynamics in proximity to the invariant manifold. For the systems (1) and (2), the dynamics can be linearized near the fixed point to obtain

$$\log X_{t+1} = \ln(A_0 + \alpha Y_t) + \ln[X_t(1 - X_t)] \approx \ln(A_0 + \alpha Y_t) + \ln X_t . \quad (15)$$

Thus the dynamics of the system close to the invariant manifold is locally a random walk in logarithmic coordinates, and this dynamics is captured by the distribution of the off phases. For this reason, a power-law distribution of quiescent phases, $P(T_\phi) \propto T_\phi^{-3/2}$, is not a sufficient condition to declare the occurence of on-off intermittency. This point is explored further in Sec. VII.

C. Power spectra

Another interesting issue concerns the shape of the power spectrum. Simple nonintermittent, chaotic systems, such as the logistic map with constant A, generate signals with power spectra that are either white or blue [18] (that is, dominated by the high-frequency components). By contrast, signals generated by on-off intermittency have red spectra with low frequencies predominating [17]. In that way, on-off intermittent systems act as nonlinear integrators that take white driving signals and transform them into red signals characterized by low-frequency variability and spectral energy growing with the wavelength. Additionally, the power spectra of on-off intermittent time series often display approximate power-law behavior with spectral energy density $P(\omega)$ proportional

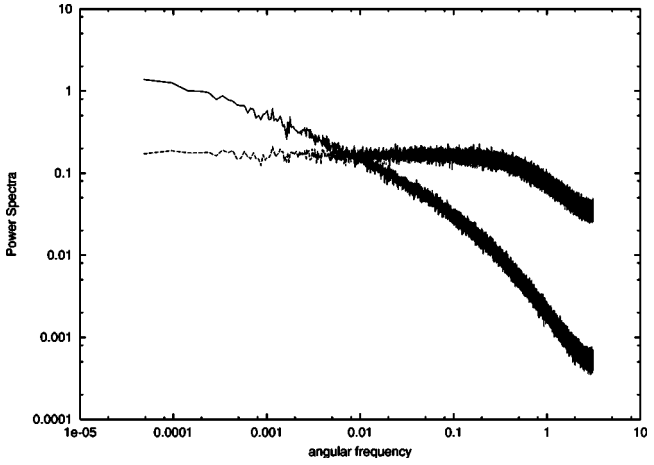

FIG. 5. Power spectra for the on-off intermittent dynamics corresponding to $A_0=0$, $\alpha=2.75$ (solid line) and for the nonintermittent dynamics corresponding to $A_0=0.5$, $\alpha=2.75$ (dashed line). The power spectra have each been obtained by averaging over 100 realizations of the process, each having a length of 2^{17} points.

to a power of the inverse of the angular frequency ω: $P(\omega)\propto 1/\omega^{\gamma}$ with γ usually smaller than 1. In Fig. 5 we contrast the power spectra for the systems (1) and (2) in a situation of on-off intermittency with that in a state of nonintermittent, noisy chaotic dynamics. The spectra have been computed for the same parameter values already considered above, and averaged over 100 realizations, each of which is composed of 2^{17} points. The two spectra are completely different, with the spectrum for nonintermittent dynamics showing a white noise behavior.

Though power-law spectra and power-law amplitude distributions have often been taken as indicators of self-organized criticality (SOC, Ref. [19]), as we see from this example, power-law statistics are also associated with on-off intermittency. Hence, the detection of power laws from measured signals does not warrant the conclusion that SOC is operating, as there are other mechanisms (including on-off intermittency) that produce such statistics.

D. Multifractal properties

In the analysis of signals, it is useful to introduce the generalized structure functions

$$S_q(\tau)\equiv(\langle|X_{t+\tau}-X_t|^q\rangle)^{1/q}, \tag{16}$$

where the symbol $\langle\cdots\rangle$ again indicates average over time, and τ is an integer delay time. When

$$S_q(\tau)\propto\tau^{H_q} \tag{17}$$

for small τ, the signal is said to have scaling and H_q is called a scaling exponent [20].

The standard structure function of a signal is S_2. Monofractal, or self-affine, signals are characterized by the equality $H_q=H_2$ for all q. Brownian motion and white noise are examples of monofractal signals, having $H_2=0.5$ and $H_2=0$, respectively. Multifractal, or multiaffine, signals are characterized by *anomalous scaling* in which $H_q>H_p$ for some positive numbers $q<p$ [21]. Multifractal signals are generated by nonlinear (deterministic or stochastic) processes, and their Fourier transforms have correlated phases [22].

Figure 6(a) shows the set of generalized structure functions for the on-off time series shown in Fig. 2(a). An approximate power-law behavior appears for the different moments, allowing for the determination of the generalized scaling exponents H_q. Figure 6(b) shows the generalized scaling exponents H_q versus q, as obtained by averaging over 100 realizations of the processs (1) and (2), by using different random seeds for the stochastic driver. The logarithmic slopes of the structure functions have been computed in the range $9\leqslant\tau\leqslant 90$. The upper and lower curves indicate, respectively, the maximum and minimum values of the scaling exponent on the ensemble of realizations. The scaling exponents decrease monotonically with the order q of the

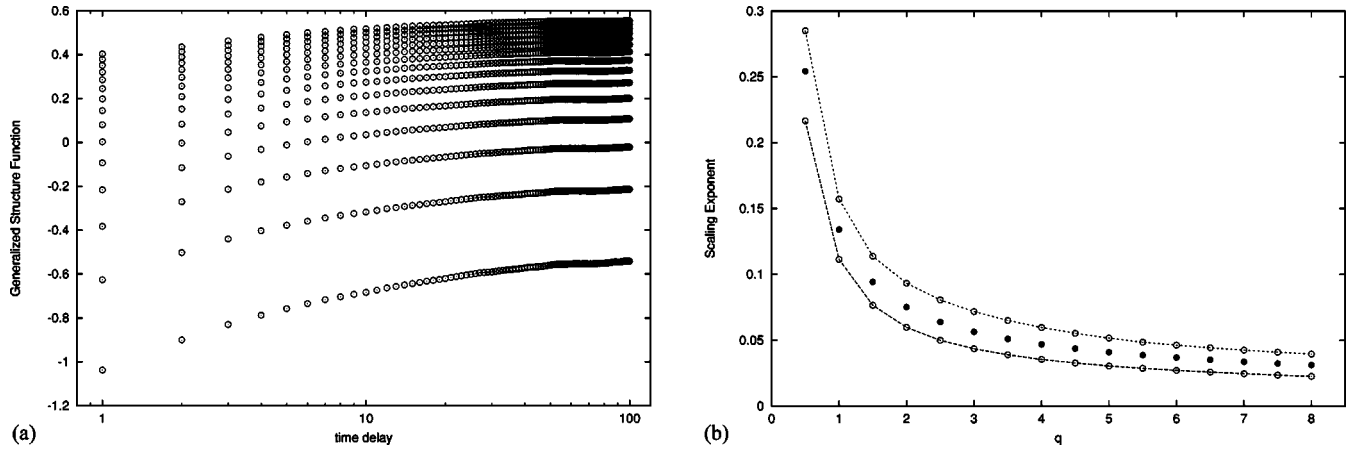

FIG. 6. (a) Generalized structure functions for moments of order $q=0.5,1,1.5,\ldots,8$ for the on-off intermittent system corresponding to $A_0=0$, $\alpha=2.75$, in ascending order. (b) Average scaling exponents, as computed by a power-law fit to structure functions in the range $9\leqslant\tau\leqslant 90$. These scaling exponents are computed as an average over an ensemble of 100 realizations. The upper and lower curves indicate, respectively, the maximum and minimum values of the scaling exponent for each moment order, as obtained from the ensemble of 100 realizations.

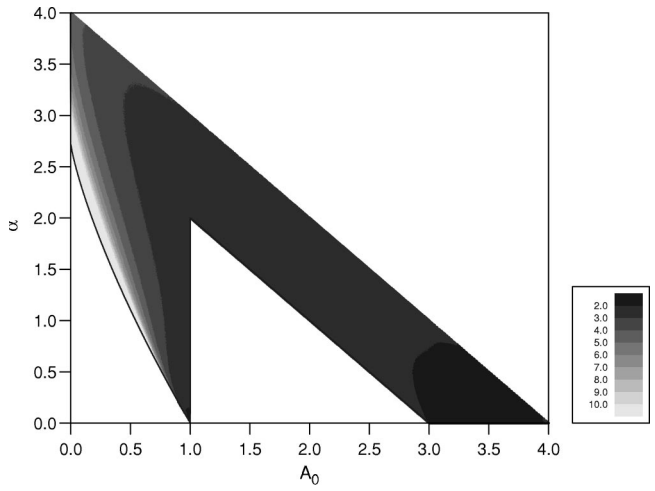

FIG. 7. The distribution of values of the kurtosis in the parameter plane. In the light portion, the values are significantly greater than 3, indicating the parameter values in which we may expect to find on-off intermittency.

moment. Analogous results are found for other parameter values that lead to on-off intermittency. Thus, Fig. 6 indicates that signals generated by on-off intermittency display anomalous scaling. By contrast, nonintermittent chaotic dynamics does not lead to structure functions with scaling properties [23].

IV. A REGIME DIAGRAM

To form a comprehensive picture of the complex of characteristics of a signal generated by on-off intermittency, we construct a regime diagram for the driven logistic map showing the region of parameter space where on-off intermittency occurs in that model. To produce the diagram, we have computed several global statistics for the part of parameter plane where intermittency is theoretically possible. In particular, we have considered the following statistics:

(1) The logarithmic slope of the power spectrum. This is negative for on-off intermittency, while it is null or positive for noisy chaotic, nonintermittent dynamics.

(2) The kurtosis of the time series. This is definitely larger than 3 for intermittent systems and it is ≈ 3 for nonintermittent dynamics.

(3) The logarithmic slope of the distribution of off phases.

All these statistical estimators provide consistent answers about where the on-off intermittency is found so, in the interests of brevity, we discuss only the results of the kurtosis analysis.

Figure 7 shows the values of the kurtosis in the parameter plane (A_0, α). The kurtosis is significantly larger than 3 only in a thin slice just above the theoretical curve (6) discussed by Heagy *et al.* The lower edge of the region of on-off intermittency coincides with this curve, while the upper edge is fuzzier and a well-defined border cannot be identified here. Intermittency is strongest immediately above the critical line and it merges smoothly with the nonintermittent noisy chaos found for larger values of the parameters. Consistently, the value of the kurtosis is largest at the critical line and it decreases for increasing values of A_0 and/or α. For given A_0, the range of values of α for which on-off intermittency is present is quite limited.

V. VARIATIONS ON THE THEME

A. Deterministic drivers

Having seen how a deterministic system parametrically driven by a stochastic process produces on-off intermittency, we may ask what happens when the driving process is deterministic. The deterministic case has already been considered in earlier studies [6,15–17] and we here recall the case of two coupled logistic maps with skew-product structure, namely,

$$X_{t+1} = A(Y_t) X_t (1 - X_t), \tag{18}$$

$$Y_{t+1} = B Y_t (1 - Y_t), \tag{19}$$

$$A(Y_t) = A_0 + \alpha Y_t, \tag{20}$$

where B is constant.

In Eqs. (18)–(20), the probability distribution function $\rho(Y)$ of the chaotic driving signal Y_t entering the integral in Eq. (7) is different from that of the noise-driven system considered previously. The lower threshold for on-off intermittency is correspondingly different. The lower limit to on-off intermittency for the chaotic driving reaches the value $\alpha_c = 4$ for $A_0 = 0$. Thus, in order to generate intermittency with this form of chaotic driving we need to have $A_0 \neq 0$.

Figure 8 shows a sample time series [panel (a)], together with the amplitude distribution [panel (b)], the power spectrum [panel (c)] and the distribution of the off phases (panel d) for $A_0 = 0.01$, $\alpha = 3.99$, and $B = 4$. For these parameter values, the system behaves very similarly to what happens with a stochastic driver, indicating that on-off intermittency does not require the presence of stochastic forcing. As discussed by von Hardenberg *et al.* [16], distinguishing between deterministic and stochastic drivers in the analysis of a time series requires either access to the extremely small scales achieved during the off periods or the explicit recognition of the phase-space structures present at large amplitudes, which are induced by the deterministic driver.

The above result was found for $B = 4$. For smaller values of B, the situation changes slightly. When $B < 4$, the driving variable Y_t is confined to a subset of the interval (0,1) that becomes smaller as the value of B decreases. Figure 9 shows the probability distribution of the driver, Y_t, for the values $B = 3.9$ and $B = 3.75$. Shrinking in the width of the distribution $\rho(Y)$ is evident. For values of B smaller than the threshold for chaos in the logistic map, $B_c \approx 1.4$, the variable Y_t is periodic or tends to a fixed point.

On account of the different distribution of the driver, $\rho(Y)$, for $B_c < B < 4$ the critical curve for the appearance of on-off intermittency moves to lower values of α. Figure 10 shows the critical curve for the cases $B = 4$, $B = 3.9$, and $B = 3.75$. As expected, on-off intermittency is present only in a

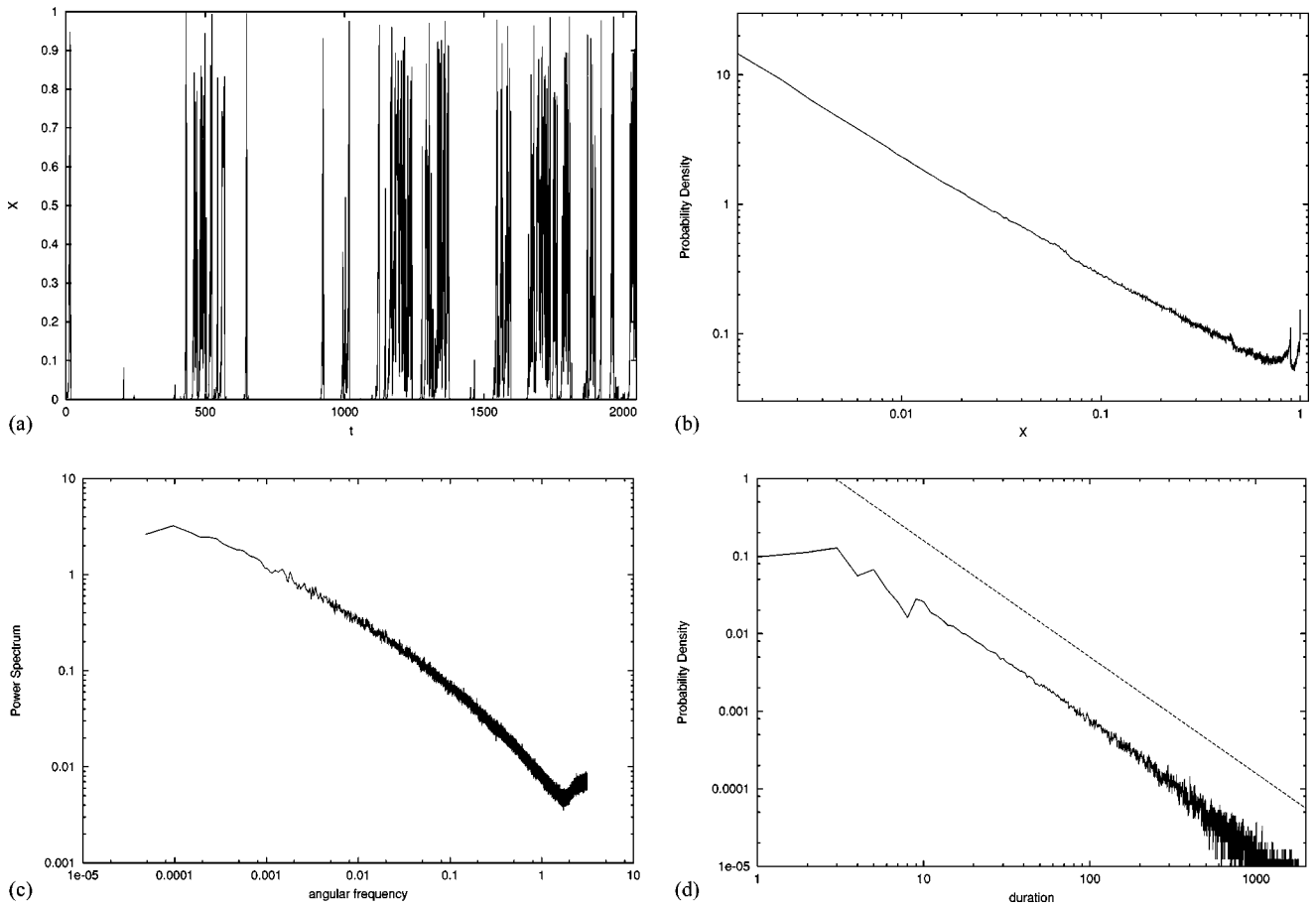

FIG. 8. Results for a chaotically forced logistic map, Eqs. (18)–(20), for the parameter values $A_0=0.01$, $\alpha=3.99$, and $B=4$. (a) Sample time series of the driven variable X_t, (b) amplitude distribution, (c) power spectrum, and (d) distribution of the duration T_ϕ of the *off* phases. The amplitude distribution and the power spectrum have been obtained by an average over 100 realizations of the process. Every realization has a duration of 2^{17} points. The distribution of the off phases has been obtained from one realization with duration 2×10^7 points. The dashed line in panel (d) indicates a power-law behavior $T_\phi^{-3/2}$.

thin region of the parameter plane just above the critical curve.

B. The effect of feedback

In the study of dynamical systems, there is often a distinction made between driven and autonomous systems. Yet it is not so hard to see either one in terms of the other. When one makes a surface of section it is really a stroboscopic map in which the variation of one coordinate is used as the clock. It may not be a good clock by some lights, but it makes for good maps. Similarly, on-off intermittency may be either driven or autonomous, the difference being that in the former

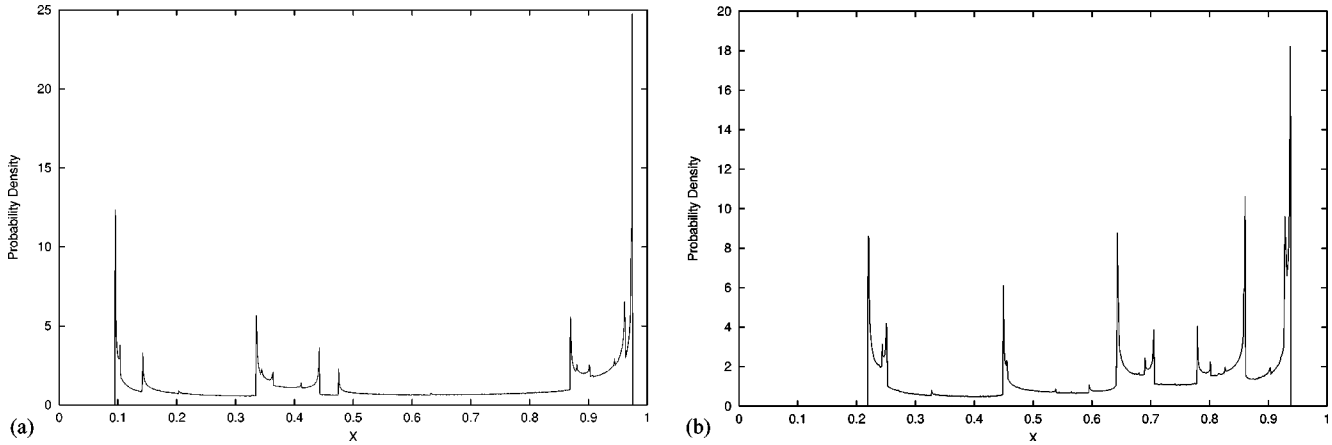

FIG. 9. Probability distribution of the chaotic driver Y_t, Eq. (19) in the text, for the values $B=3.9$ [panel (a)] and $B=3.75$ [panel (b)].

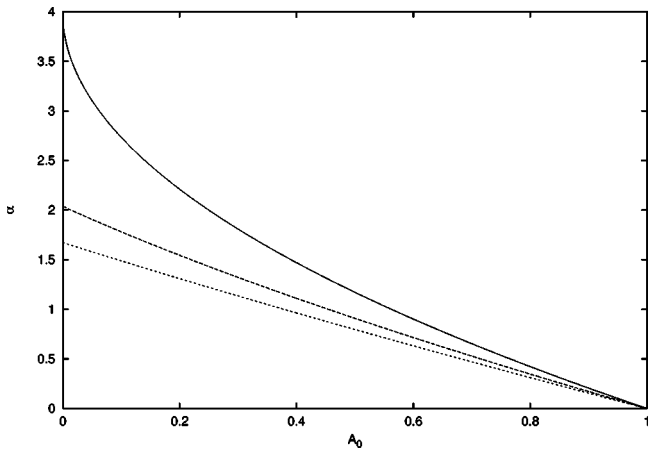

FIG. 10. Critical curve for the onset of on-off intermittency with a chaotic driver, Eq. (19) in the text, for the cases $B=4$, $B=3.9$, and $B=3.75$.

case we have the so-called skew-product structure that, as we have suggested, is useful for constructing models. However, the earliest models of the process did not have this feature, which, in fact, is not essential for the functioning of the mechanism [7].

A simple example of autonomous on-off intermittency, that has been given before [6,7], is the model system

$$X_{t+1}=(A_0+\alpha Y_t)X_t(1-X_t), \tag{21}$$

$$Y_{t+1}=(B_0+\beta X_t)Y_t(1-Y_t), \tag{22}$$

where β measures the intensity of the feedback. In Fig. 11 we show a time series, together with the amplitude distribution, power spectrum and distribution of the off phases for $A_0=0$, $\alpha=2.05$, $B_0=3.9$, and $\beta=0.1$. With this weak feedback, the system displays on-off intermittency. With a larger feedback (i.e., for a larger value of the ratio β/B_0), the system ceases to be intermittent and apparently undergoes nonintermittent chaotic dynamics. Here again, we see that (a) on-off intermittency is a robust feature that does not depend on the details of the driving mechanisms and (b) it is a type of behavior that is observed only in a limited parameter range located between regular behavior and full-blown chaotic dynamics.

Finally, we note that the mechanisms for bursting which are substantially similar to on-off intermittency, such as ''bubbling'' [11], lead to completely analogous results.

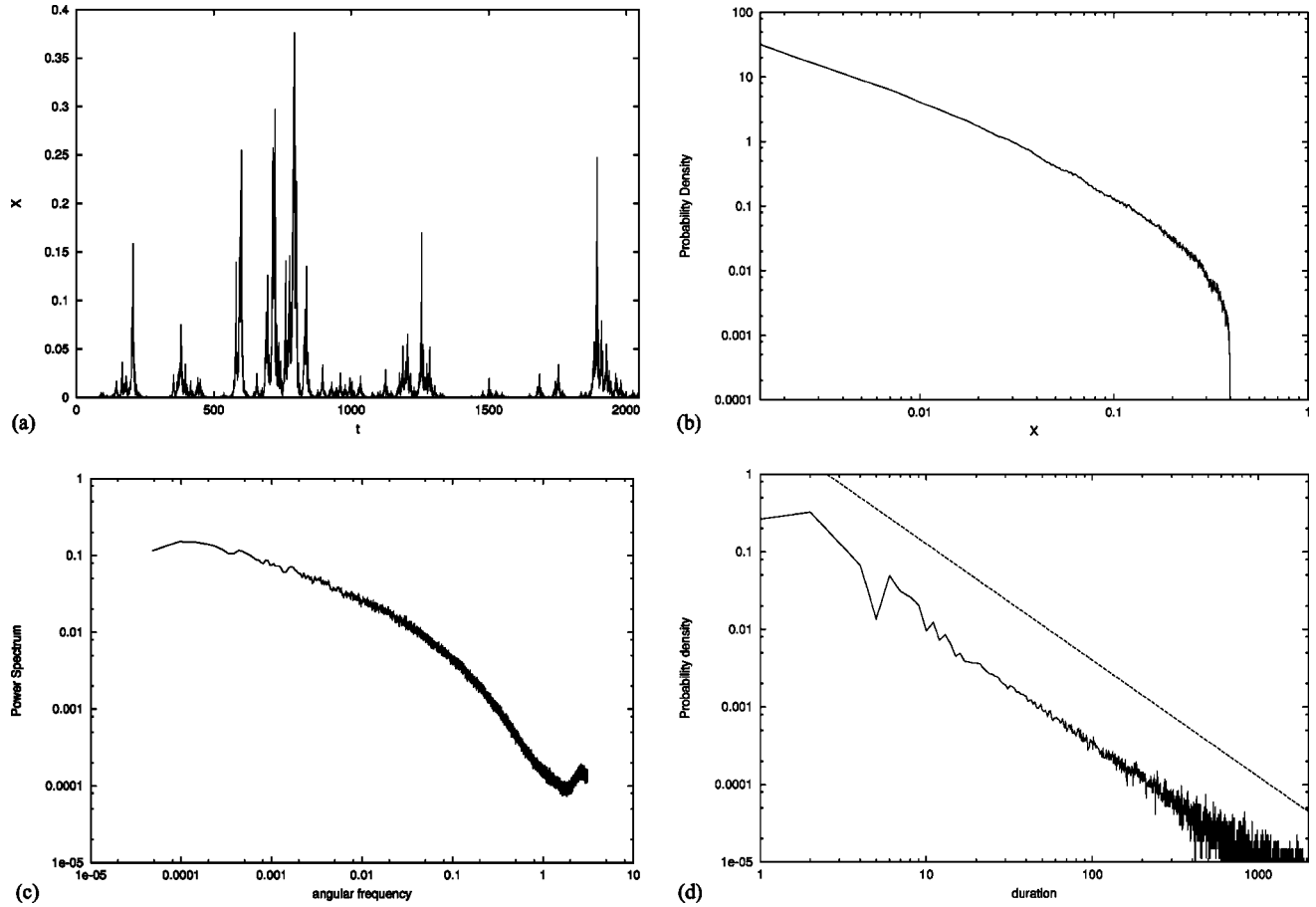

FIG. 11. Results for a chaotically forced logistic map with feedback, Eqs. (21) and (22), for the parameter values $A_0=0$, $\alpha=2.05$, $B_0=3.9$, and $\beta=0.1$. (a) Sample time series of the driven variable X_t, (b) amplitude distribution, (c) power spectrum, and (d) distribution of the duration T_ϕ of the *off* phases. Same details as in Fig. 8.

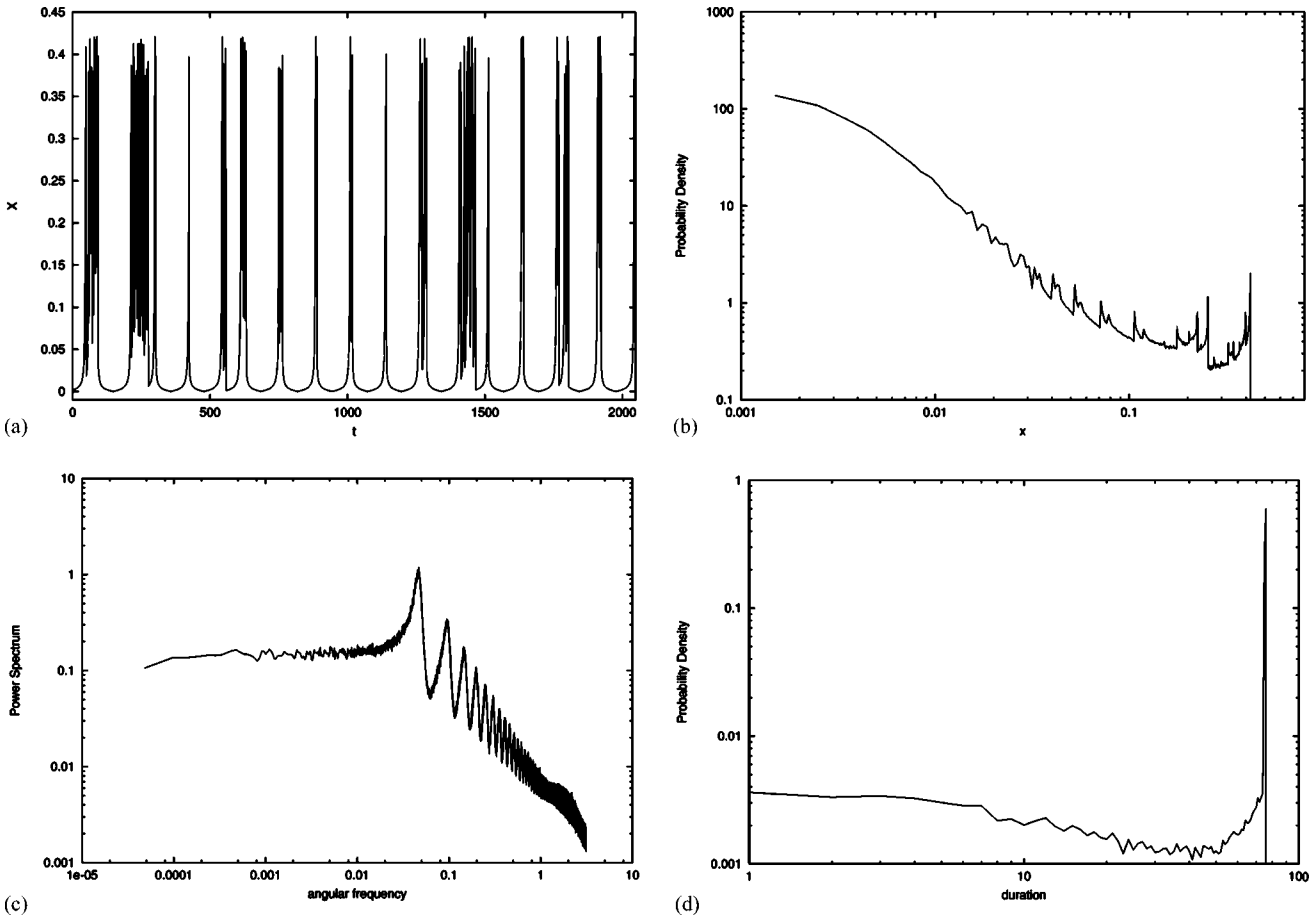

FIG. 12. Results for a system undergoing Pomeau-Manneville intermittency, Eq. (23), for the parameter values $a=-42.39$, $b=84.27$, $c=-54.3$, and $d=12.43$. (a) Sample time series of the state variable X_t, (b) amplitude distribution, (c) power spectrum, and (d) distribution of the duration T_ϕ of the *off* phases. Same details as in Fig. 8.

VI. OTHER FORMS OF INTERMITTENCY

Bursting signals can be generated by a diversity of mechanisms. In the previous sections, we have identified some of the signatures of on-off intermittency and its variants, in order to be able to detect them in the analysis of measured time series. Here, we consider some of the other standard processes that produce bursting, and we show that they can be easily distinguished from on-off intermittency on the basis of the statistical properties of the signals that they generate.

A process that generates bursting signals is the Pomeau-Manneville mechanism. This type of intermittency is observed for maps of the interval whose graphs, in some region of their domains of definition, pass very close to the 45 deg line without crossing it. In this case the near intersection of the map with the 45 deg line produces a virtual fixed point analogous to the second fixed point that we mentioned for the case of on-off intermittency. The difference is that, for on-off intermittency, the second fixed point controls the bursting, whereas the ghost point in the Pomeau-Manneville scenario is the producer of quiescent behavior. Both mechanisms produce bursty signals but with different statistical properties as we now explain.

As an example of Pomeau-Manneville intermittency, we consider the map given by

$$X_{t+1}=f(X_t)=aX_t^4+bX_t^3+cX_t^2+dX_t, \tag{23}$$

defined in $0\leqslant X_t<1$. In the following illustration, we use $a=-42.39$, $b=84.27$, $c=-54.3$, and $d=12.43$. The values of the parameters are chosen so as to have a point of near tangency—we are tempted to call it a point of pretangency. If this point is at $X_{tan}=0.5528$ its image is $f(X_{tan})=0.5529$, while the difference between the point and its image is $|f(X_{tan})-X_{tan}|=10^{-4}$. For this model, if we may measure activity $\mathcal{N}$ as the distance from the point X_{tan}, then the off phases correspond to the periods when the system is in the neighborhood of X_{tan}. For comparison of the behavior with that of on-off intermittency, we thus consider the signal $X_t'\equiv\mathcal{N}(X_t)=|X_t-X_{tan}|$.

Figure 12(a) shows an example of the behavior of $X_t'=|X_t-X_{tan}|$ for the above parameter values. The variable X_t' spends long periods close to zero, with rapid excursions far from this point. Figure 12(b) shows the amplitude distribution of the signal X_t', as obtained from an ensemble of 100 realizations of the process, each composed by 2^{17} points. Although a power-law behavior is not present, this distribu-

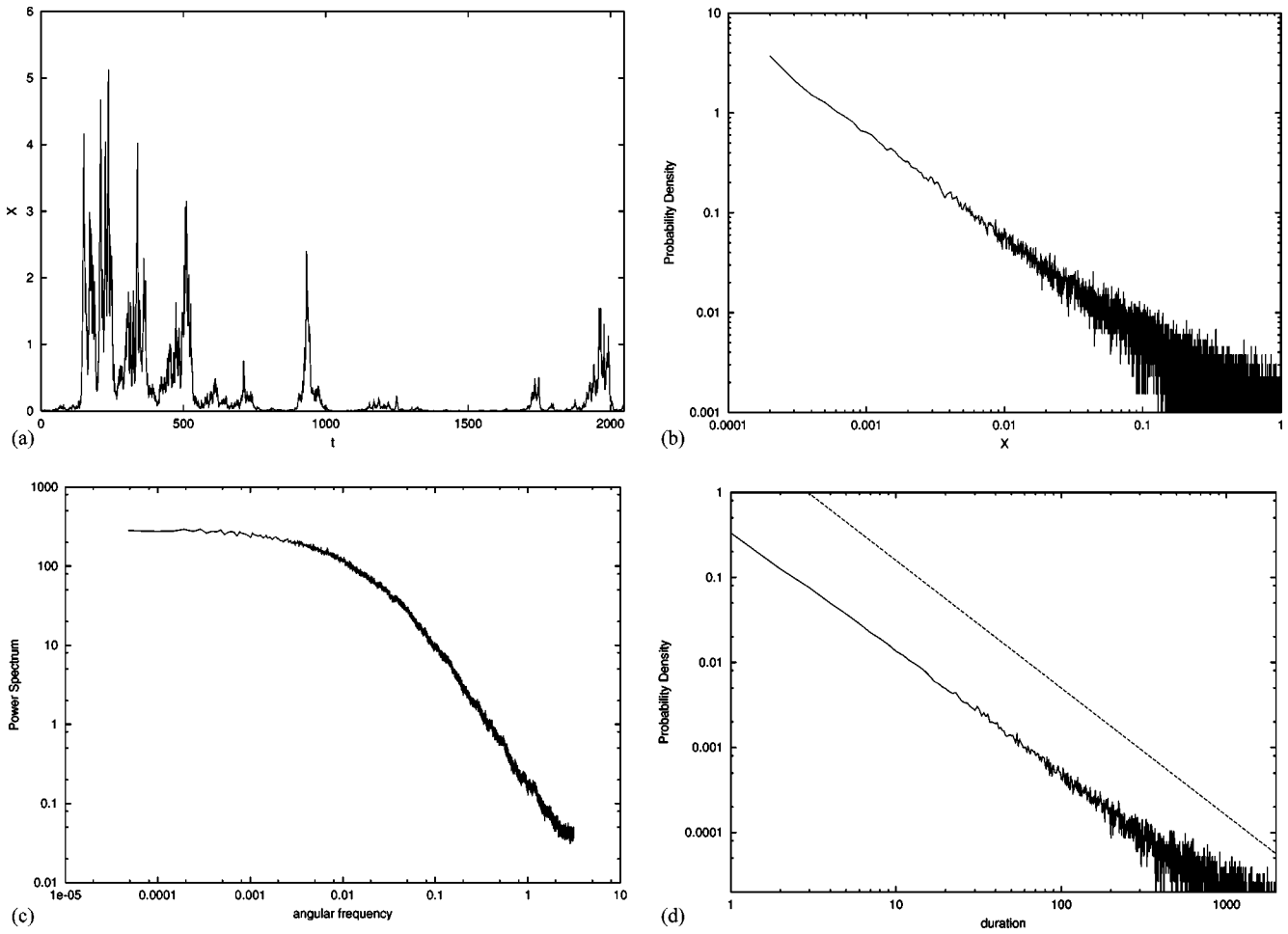

FIG. 13. Results for the nonlinearly filtered, linear autoregressive AR(1) process discussed in the text, Eq. (25). (a) Sample time series of the state variable X_t, (b) amplitude distribution, (c) power spectrum, and (d) distribution of the duration T_ϕ of the *off* phases. The threshold for determining the lengths T_ϕ of the off phases has been set to 0.001. Same details as in Fig. 8.

tion is not so different from that generated by on-off intermittency, and the two could probably be confused with each other in the analysis of experimental signals affected by measurement errors.

Figure 12(c) shows the power spectrum of the signal X_t', again obtained by an average over 100 realizations of 2^{17}-point-long time series. The power spectrum has an average power-law appearance only at high frequency, while it becomes flat at low frequency. This behavior is quite different from what is observed for on-off intermittency.

The most striking difference between the intermittent behavior generated by the Pomeau-Manneville scenario and on-off intermittency is found in the distribution of the durations of off phases. Figure 12(d) shows the distribution of the duration T_ϕ of the periods for which $X_t' < 0.005$. The distribution of T_ϕ peaks at a given maximum value, as can be qualitatively gathered from the inspection of Fig. 12(a). This behavior is totally different from the power-law behavior, $T_\phi^{-3/2}$, obtained for on-off intermittency.

Analogous results are obtained for different values of the parameters in map (23), or for different maps having a similar behavior of quasitangency to the 45 deg line. By computing the power spectrum and, above all, the distribution of off phases of a measured signal, the Pomeau-Manneville intermittent scenario can be easily distinguished from on-off intermittency.

Before closing this section we recall that simple unimodal, one-dimensional maps can generate bursting behavior. One example is the map introduced by Maynard-Smith [24] in the context of population dynamics,

$$X_{t+1} = \frac{rX_t}{1+(aX_t)^b}, \tag{24}$$

where a, b, and r are control parameters taken to be positive. At small X, the map has slope r. At larger X, the map reaches a maximum, after which it decreases toward zero. For large values of b, the map is very steep in the decreasing portion beyond the maximum and it is said to have an *overcompensating* behavior. For large b, this map can produce intermittent-looking signals, having a red power spectrum at high frequencies [25]. These signals have statistical properties that are similar to those produced by the Pomeau-Manneville mechanism, and they can be easily distinguished from signals produced by on-off intermittency on the basis of the distribution of quiescent phases.

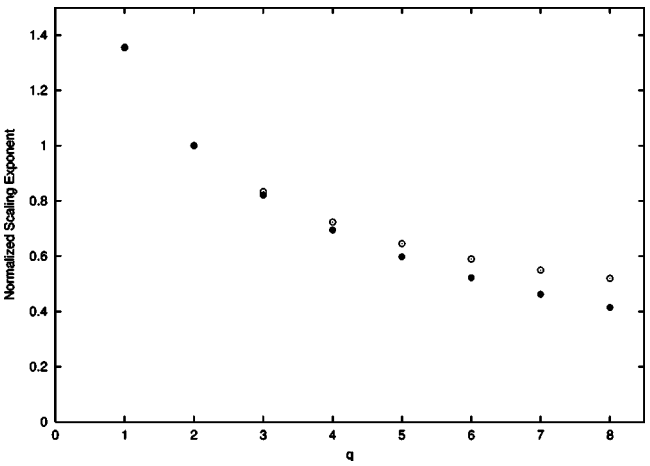

FIG. 14. Generalized scaling exponents for on-off intermittency (filled circles) and for the nonlinearly filtered, linear autoregressive AR(1) process discussed in the text, Eq. (25) (empty circles). The scaling exponents have been normalized by dividing them for the value of the second-order exponent, H_2.

VII. A TRANSFORMATION OF VARIABLES

The mechanisms for bursting discussed above can all be associated with specific phase-space dynamical features. However, bursting signals can be simply generated by taking a nonlinear transformation of a linear autoregressive process [FLAP (filtered linear autoregressive process)]. The analysis that follows indicates that a FLAP can mimic the output of the on-off intermittency, insofar as scaling is concerned.

To be specific, we consider the process [26]

$$Z_{t+1}=C_1Z_t+\sigma W_t, \quad X_{t+1}=C_2\exp(Z_{t+1}), \qquad (25)$$

where $C_1=0.999$, $C_2=0.001$, and $\sigma=0.5$. Here W_t is white noise uniformly distributed between -1 and 1. Figure 13(a) shows a sample time series for this process, Fig. 13(b) shows the amplitude distribution, Fig. 13(c) shows the power spectrum, and Fig. 13(d) shows the distribution of the duration of the off phases. The distribution of T_ϕ has a power-law dependence, $p(T_\phi)\propto T_\phi^{-3/2}$, as observed for on-off intermittency.

For this process, the amplitude distribution has a power-law dependence and the power spectrum has an approximate power law dependence at high frequencies. In addition, the distribution of T_ϕ has a power-law dependence, $p(T_\phi)\propto T_\phi^{-3/2}$, as observed for on-off intermittency. In fact, this behavior is related to the basic properties of Brownian motion: as shown by Heagy *et al.* [15], the distribution of the off phases depends only on the linearized dynamics of the process. Since a simple linear AR(1) process passed through a nonlinear static filter can generate a power-law distribution for the duration of off phases, this property is clearly not enough to guarantee the presence of on-off intermittency or of other dynamical behaviors, such as SOC.

Indeed, we observed that even the multifractal properties are not sufficient to distinguish between the different processes. For example, a δ-correlated stochastic process with exponential amplitude distributions can lead to the appearance of multifractality when the data are analyzed with box-counting methods [27]. Discreteness effects, lack of statistics, and nonlinear static filters acting on linearly correlated processes (such as taking the exponential of a linear autoregressive process) can lead to a decrease of H_q with increasing q. In the present case, the interplay of linear correlations and of a nonlinear static transformation leads to a multifractal behavior of the signal produced by the FLAP (25). To illustrate this behavior, we show in Fig. 14 the generalized scaling exponents for an on-off signal of the type discussed above and for a signal coming from the FLAP (25). The scaling exponents have been normalized by dividing them for the value of the second-order exponent, H_2, since the two signals have slightly different linear correlations (measured by H_2), while what is of interest here is the relative decrease of the scaling exponent from its value for $q=2$. The behavior of the two signals is similar and a clear distinction between finite-length signals generated by the two processes cannot be drawn on this basis.

VIII. DISCUSSION AND CONCLUSIONS

We have seen how on-off intermittency is produced by a logistic map whose control parameter fluctuates, either chaotically or stochastically. The method of making parameters vary is an effective way of producing chaos as well as on-off intermittency. The resultant behavior in turn depends on the parameters controlling the variations in the original parameter itself [3].

What the model reveals is that in a sliver of the parameter space that controls the ''variable parameter'' itself, we find on-off intermittency. This sliver is a transition layer from order to chaos lying just above the critical curve determined by Heagy *et al.* [15]. Within this surprisingly limited region, we find a number of telltale characterisitics of signals produced by on-off intermittency. It is interesting that passage through this narrow strip of parameter space is a route to chaos for the system just as for other intermittencies, notably the Pomeau-Manneville varieties. On one side of the parameter strip of on-off intermittency, the system undergoes chaotic, nonintermittent dynamics driven by external parametric noise (if we may call a nondeterministic system chaotic) and, on the other side, it is in a stable quiescent state. The route to chaos for this system is through the parametric territory of on-off intermittency.

A further result of this study concerns the possibility of distinguishing on-off intermittency from other bursting mechanisms. As we have shown, the statistical properties that we have considered are sufficient to distinguish on-off intermittency from other mechanisms for bursting, such as the Pomeau-Manneville intermittency scenario and the behavior of an overcompensatory bursting map.

On the other hand, we have shown that a simple FLAP, i.e., a linear autoregressive process passed through a nonlinear static filter, generates time series that mimics many of the properties of on-off intermittent signals. In particular, such signals have a power-law distribution of the duration of off phases, $P(T_\phi)\propto T_\phi^{-3/2}$, and display apparent multifractal behavior when studied with standard analysis methods. We

have so far been unable to find any statistical criteria for making a clear distinction between signals generated by on-off intermittency and signals generated by nonlinear filtering of autoregressive processes, although we cannot exclude the possibility that such a statistical criterion could exist.

ACKNOWLEDGMENTS

We are grateful to Luca Ferraris for useful discussions. We acknowledge the financial support of NSF under Grant No. DMS-99-72022.

[1] G. Batchelor and A. Townsend, Proc. R. Soc. London, Ser. A **199**, 238 (1949).
[2] N. Platt, E. Spiegel, and C. Tresser, Geophys. Astrophys. Fluid Dyn. **73**, 147 (1993).
[3] E. Spiegel, in *Past and Present Variability of the Solar-Terrestrial System: Measurement, Data Analysis and Theoretical Models*, edited by G. Cini Castagnoli and A. Provenzale (IOS Press, Amsterdam, 1997).
[4] J. Maurer and A. Libchaber, J. Phys. (France) Lett. **41**, 515 (1980).
[5] Y. Pomeau and P. Manneville, Commun. Math. Phys. **74**, 189 (1980).
[6] N. Platt, E.A. Spiegel, and C. Tresser, Phys. Rev. Lett. **70**, 279 (1993).
[7] E.A. Spiegel, Ann. N.Y. Acad. Sci. **617**, 305 (1981).
[8] A.S. Pikovsky, Z. Phys. B: Condens. Matter **55**, 149 (1984).
[9] H. Fujisaka and H. Yamada, Prog. Theor. Phys. **75**, 1087 (1986).
[10] P. Ashwin, J. Buescu, and I.N. Steward, Phys. Lett. A **193**, 126 (1994).
[11] S.C. Venkataramani, B.R. Hunt, and E. Ott, Phys. Rev. E **54**, 1346 (1996).
[12] E. Ott and J.C. Sommerer, Phys. Lett. A **188**, 39 (1994).
[13] P. Ashwin, E. Covas, and R. Tavakol, Nonlinearity **9**, 563 (1999).
[14] E. Knobloch and J. Mohelis, in *Nonlinear Instability, Chaos and Turbulence*, edited by L. Debnath and D. Riahi (Computational Mechanics, Southampton, 2000), Vol. II.
[15] J.F. Heagy, N. Platt, and S.M. Hammel, Phys. Rev. E **49**, 1140 (1994).
[16] J. von Hardenberg, F. Paparella, N. Platt, A. Provenzale, E.A. Spiegel, and C. Tresser, Phys. Rev. E **55**, 58 (1997).
[17] N.J. Balmforth, A. Provenzale, E.A. Spiegel, M. Martens, C. Tresser, and C.W. Wu, Proc. R. Soc. London, Ser. B **266**, 311 (1999).
[18] J.E. Cohen, Nature (London) **378**, 610 (1995).
[19] P. Bak, C. Tang, and K. Wiesenfeld, Phys. Rev. Lett. **59**, 381 (1987).
[20] U. Frisch, *Turbulence* (Cambridge University Press, Cambridge, 1995).
[21] G. Paladin and A. Vulpiani, Phys. Rep. **156**, 147 (1987).
[22] R. Vio, S. Cristiani, O. Lessi, and A. Provenzale, Astrophys. J. **391**, 518 (1992).
[23] A. Provenzale, L.A. Smith, R. Vio, and G. Murante, Physica D **58**, 31 (1992).
[24] J. Maynard-Smith, *Models in Ecology* (Cambridge University Press, Cambridge, 1974).
[25] A. Blarer and M. Doebeli, Nature (London) **380**, 589 (1996).
[26] H. Tong, *Non-linear Time Series: A Dynamical System Approach* (Clarendon Press, Oxford, 1990).
[27] J. von Hardenberg, R. Thieberger, and A. Provenzale, Phys. Lett. A **269**, 303 (2000).